Hindawi
International Journal of Polymer Science
Volume 2022, Article ID 7816333, 11 pages
https://doi.org/10.1155/2022/7816333

Research Article

Structural and Physicomechanical Properties of an Active Film Based on Potato Starch, Silver Nanoparticles, and Rose Apple (*Syzygium samarangense*) Extract

Raj Kumar,[1] Naina Gautam,[2] Shashikant Yadav,[2] T. Venketesh,[3] and Nasir Awol[4]

[1]*CSIR-Central Building Research Institute (CSIR-CBRI), Roorkee, Uttrakhand 247667, India*
[2]*Dr. B. R. Ambedkar National Institute of Technology, Grand Trunk Road, Barnala-Amritsar Bypass Rd., Jalandhar, Punjab 144011, India*
[3]*CSIR-National Institute for Interdisciplinary Science and Technology (CSIR-NIIST), Trivandrum, Kerala 695019, India*
[4]*Department of Physics, Hawassa University, Hawassa, Ethiopia*

Correspondence should be addressed to Nasir Awol; nasirawol1@gmail.com

Received 18 December 2021; Revised 13 March 2022; Accepted 7 May 2022; Published 10 June 2022

Academic Editor: Yulin Deng

In the current research work, active films were made from potato starch (PS) and AgNP solution comprising of silver nanoparticles (AgNPs) and rose apple extract (RE) via the casting method at various concentrations. AgNP solution in the PS matrix significantly altered the physical properties such as opacity, water vapor permeability mechanical property, solubility, and swelling index of the films. The influence of AgNP solution on the properties of the films was deeply examined. The results found that the 15% AgNP solution films exhibited better physicochemical properties. The presence of AgNP solution in the PS matrix significantly improved the properties of active films which is evident from the results of FTIR and SEM. Results show that AgNPs and PS were uniformly mixed and formed continuous and homogenous films without bubbles and cracks. In addition, the AgNP solution in the films significantly improved the antibacterial activity against *S. aureus* than *P. aeruginosa* in the films.

1. Introduction

Excessive use of packaging materials derived from petroleum-based sources for a wide range of applications such as food, pharmaceutical, and other applications have led to environmental degradation and pollution. Worldwide, scientists focus on developing environmentally friendly and cost-effective polymeric materials which can potentially replace synthetic polymers [1]. Therefore, the sustainable packaging materials derived from various natural polymers such as cellulose, starches, proteins, and lipids have gradually attracted scientists' and academicians' attention and they have successfully utilized them to develop biodegradable packaging materials [2]. Many studies have been published on natural polymers like proteins, lipids, and starch to create biodegradable packaging materials [3, 4]. Starch-based packaging materials attracted particular attention due to their abandoned nature and excess availability, excellent film-forming property, biodegradability, low cost, and nontoxic nature. However, starch does not show the significant functional properties required for selective applications [5]. Hence, an attempt has been made to incorporate AgNPs along with the starch matrix for boosting the functional properties of the film, quality, and eventually shelf life of food materials.

Reinforcing agents, including nanofillers with high surface area, exhibit excellent interactions within the polymer matrix which was found to improve the functional properties of the polymers. In the last few years, many nanofillers, including ZnO, TiO_2, ZnO, and AgNPs, have been tried to develop nanocomposite materials with improved functional properties like mechanical, optical, moisture resistance, and antibacterial [6]. This nanofiller imparted the strength of the films and confers the power to fight against microorganisms, which unfold the ways for creating cost-effective food

packaging materials [7]. Some works of literature have suggested that nanofillers enhanced the fundamental properties of the nanocomposite materials and added new features like antioxidants and antibacterial [8, 9]. Recently, some studies in the literature suggested that adding plant extracts enhanced the functional properties of the natural polymer-based films which helped extend the shelf life as well as the quality of food but improvement in functional properties still remains a challenge [10–12]. To prepare nanoparticles, either the chemical or the green method was used. Both techniques show some advantages in themselves. But the toxicity problem cannot be obviated in the chemical method. In the green process, reducing agents used in the green process come from the plants. It is also noted that the green technique is more economical than the chemical method [13].

However, we preferred the green approach to prepare the AgNP solution using guava leaf extract as a reducing agent in the present work. As a reducing agent, different parts of guava (*Psidium guajava* L.) have been utilized traditionally to treat various diseases, including gastroenteritis and diarrhea. Many works have shown that the quercetin content in leaf extract in flavonoids acted as an excellent antibacterial activity [13]. AgNPs have various applications, like sensors, wastewater, and pharmaceuticals [14]. Therefore, if AgNP solution is added to PS films, it shows excellent antibacterial activity and functional properties, owing to their AgNPs, flavonoids, and polyphenol contents. In the current study, we prepared PS films with AgNP solution and evaluated functional properties. In addition, the applicability of the prepared films as an antibacterial packaging material was assessed by evaluating the antibacterial activities of the films [15].

2. Materials and Methods

2.1. Materials. PS, calcium chloride, sorbitol, antibiotics (rifampicin), bacteriological agar, and silver nitrate were obtained from Loba Chem, HiMedia, and Nice Chemicals (India). Bacterial strains such as *P. aeruginosa* and *S. aureus* were obtained from the CSIR-Institute of Microbial Technology (IMTECH), Chandigarh, India.

2.2. Methods

2.2.1. Synthesis of AgNP Solution. AgNP solution was prepared according to Kumar et al. (2017) who reported the ecofriendly method. $AgNO_3$ solution (0.01 M) and RE were initially mixed using a magnetic stirrer. After a few minutes, silver nanoparticles (AgNPs) started forming in the solution. Because of this, the color of the solution changed from deep-brown to light-yellow. Standard approaches were utilized to isolate AgNPs from the solution.

2.3. Characterization of Silver Nanoparticles. Characterization of AgNPs was carried out by using visual observation and also various techniques. Reaction progress was monitored with time using a UV–visible spectrophotometer (Shimadzu, UV-2600) in the wavelength range (λ) 400–450 nm. The XRD analysis of biosynthesized AgNPs was studied using an X-ray diffractometer (XRD) (X'Pert PRO, Panalytical, Netherlands) with Cu Kα radiation ($\lambda = 0.1546$ nm) in the 2 theta (10°–90°). Identification of an interaction between molecules in the solution was analyzed by using a Fourier transform infrared spectroscopy (Shimadzu-8400, Japan). The FTIR spectrum was taken at a spatial resolution of 4 cm^{-1} in the reflectance mode, between 4000 cm^{-1} and 500 cm^{-1}. The shape of AgNPs and distribution was studied by using FESEM in scales of 500 nm and 10 nm.

2.4. Fabrications of the Films. Green synthesized AgNPs were mixed into 100 mL of RE according to the reported study by [16] to prepare the AgNP solution. Different concentrations (5%, 10%, 15%, and 20% *v*/*v*) of AgNP solution were integrated into the starch solution (3% *w*/*v*), designed according to the reported method by Gautam et al. [17]. A magnetic plate was used to heat solutions at 90 ± 1°C for 30 minutes. Solutions (15 mL) were cast into the plastic plates and dried at room temperature. After peeling, prepared films were stored in an airtight bag at room temperature.

2.5. Thickness. Five random locations were marked on the surface of the film to measure the thickness using a digital micrometer (Mitutoyo, Japan) with an accuracy of 0.001 mm.

2.6. Moisture Content (MC). Integrated moisture in the microstructure of the samples was investigated and represented in terms of MC. Initially, the weight (W_i) of the sample was noted down and then kept at 105 ± 1°C for 24 h. The weight of dried samples was again measured (W_f). Variations in the samples' weight were represented in terms of the moisture content and determined using equation (1) as follows:

$$\text{Moisture content}(\%) = \frac{W_i - W_f}{W_i} * 100, \quad (1)$$

where W_i and W_f are the initial weight and dried weight of film samples, respectively.

2.7. Solubility (S). First, all dried samples with the initial weight (W_0) were soaked into water and kept at 25 ± 1°C for 24 h. Insoluble samples were carefully drained from the water and again held at 105 ± 1°C for 24 h and again weighed (W_1). Finally, the *S* was estimated according to equation (2) as follows:

$$S(\%) = \frac{W_0 - W_1}{W_0} * 100, \quad (2)$$

where W_0 and W_1 are the initial dried weight and insoluble sample weight, respectively.

2.8. Water Vapor Permeability (WVP). WVP of the films was determined according to ASTM E96/E96M-16. In short, the mouths of modified glass beakers (1.2 cm diameter and a depth of 4.5) filled with dried calcium chloride (105 ± 1°C for 24 h) were closed with the samples and firmly sealed using vacuum grease. All beakers are shifted into a desiccator. The desiccator partially filled with distilled water was again moved into an oven and kept at 25 ± 1°C. Any changes in the weight were noted down in the fixed time scale. WVP of the samples was evaluated using equation (3) as follows:

$$\text{WVP} = \frac{(\Delta W/t) * X}{A(P_1 - P_2)}, \tag{3}$$

where $\Delta W/t$ is the rate of weight gain, x is the film thickness, A is the sample area, and $P_1 - P_2$ is the pressure difference across the modified glass beakers.

2.9. Opacity. The opacity (OP) of the samples was estimated using a Hunter Lab Colorimeter (ColorFlex EZ, Hunter Lab, and the USA). Calibration was done using white and black plates. OP was determined using equation (4) as follows:

$$\text{OP} = \frac{\text{OP}_\text{w}}{\text{OP}_\text{b}} * 100, \tag{4}$$

where OP_b and OP_w are opacity at black and white backgrounds, respectively.

2.10. Swelling Index (SI). Predried samples with the initial weight (M_D) shifted into a beaker containing distilled water at 25°C for 2 min. Excess moisture from the wet samples was carefully withdrawn. The weights of wet samples were again measured and represented as a M_s. The SI% was measured using the following equation (5) as follows:

$$\text{SI}(\%) = \frac{M_S - M_D}{M_D} * 100. \tag{5}$$

2.11. Mechanical Property. Mechanical properties of the films were estimated according to modified ASTEM D 882-91 using a calibrated Texture Analyzer (TA) (XT Plus, Stable Microsystems). Prepared samples were mounted one by one between the test holder grips. Mechanical grip separation, crosshead speed, and load cell were fixed to 50 mm, 0.5 mm/min, and 5 kg, respectively. Maximum strength (MS) and elongations at break (E%) were measured according to equation (6) as follows:

$$\begin{aligned} \text{Maximum strength} &= \frac{F}{A}, \\ \text{Elongation at break} &= \frac{X_1 - X_2}{X_1} * 100, \end{aligned} \tag{6}$$

where F,A, X_1, and X_2 are the maximum force, the area of film, the initial, and final gapes in grips, respectively.

2.12. Hydrophilicity. The sessile drop technique measured the films' contact angle (CA). According to the approach, a 5 μL water droplet was kept on the surface of the films. Droplet images were then captured which was utilized to calculate the CA.

2.13. UV–vis Spectroscopy. A UV–visible spectrophotometer (Shimadzu, UV-2600) was used to record UV-vis spectra of films. The spectra in the range (λ) of 200–700 nm were taken of the films.

2.14. FTIR Analysis. FTIR spectra with a resolution of 4 cm^{-1} in the range of 400–4000 cm^{-1} were evaluated to investigate the possible interactions in the films.

2.15. XRD Analysis. The XRD analysis of the film was recorded using an X-ray diffractometer (XRD) (X'Pert PRO, Panalytical, Netherlands) with Cu Kα radiation ($\lambda = 0.1546$ nm) in a 2 theta range from 10° to 90°.

2.16. SEM Analysis. An SEM (JEOL JCM-6000 Benchtop, JEOL Ltd., Japan) was employed to study the changes in the microstructure in the films. Images were captured in the magnification range of 200–1000 cm^{-1} with a spot size of ~2 nm. An accelerating voltage of 10 kV during the experiment was maintained throughout.

2.17. Antimicrobial Activity of the Films. The antimicrobial activity of the PS film with AgNP solution against *P. aeruginosa* and *S. aureus* was studied with an agar plate diffusion approach, as reported by Kumar et al. [18]. For this purpose, film-forming solution (200 mg/mL) was poured into a well (6 mm diameter) on the Mueller-Hinton Agar plate with 10^5 colony forming unit (CFU)/ml cell density which was incubated for 24 h at 37°C. The antibacterial effect of the film-forming solution was estimated in terms of the diameter of the inhibition zone.

2.18. Statistics Analysis. The prepared films' functional properties, namely, thickness, OP, SI, MC, WVP, MS, and E%, were studied using Origin 8 Pro. The difference at $P = 0.05$ was assumed to be significant.

3. Results and Discussion

3.1. AgNP Characterization. AgNPs were synthesized according to the reported approach by [18] using plant extract as a reducing agent [18]. Identification of biomolecules in plant extract which are responsible for the reduction of silver ions to silver nanoparticles was analyzed using FTIR spectra as observed in Figure 1(a). The peaks at 3318, 1635, and 1032 cm^{-1} were observed in the IR spectra of AgNPs which are related with the –O-H linkage, which shows an indication for assuming polyphenols,N-H stretching vibration in amide groups of protein or C-O deformation in the alcoholic groups, respectively. The last peaks at 1032 cm^{-1} indicated that glycoside or ether (C–O–C) groups are present in AgNPs. Plant extract contains many functional groups which are related to flavonoids and carotenoids that are responsible for the reduction of silver ions into silver nanoparticles. Figure 1(b) indicates the XRD diffraction spectrum of AgNPs. From XRD results, it was found that the AgNP spectrum has a face-centered cubic structure. A similar lattice structure pattern was reported by [19, 20]. Four major peaks at 32.40, 38.29, 46.40, 64.63, and 77.34° were found which belong to lattice plan values at 111, 200, 220, and 311 [21]. The morphology of AgNPs was captured using FESEM as shown in Figure 1(c). From the image, we can observe the uniform distribution of AgNPs which are approximately spherical, uniformly distributed, and small agglomeration.

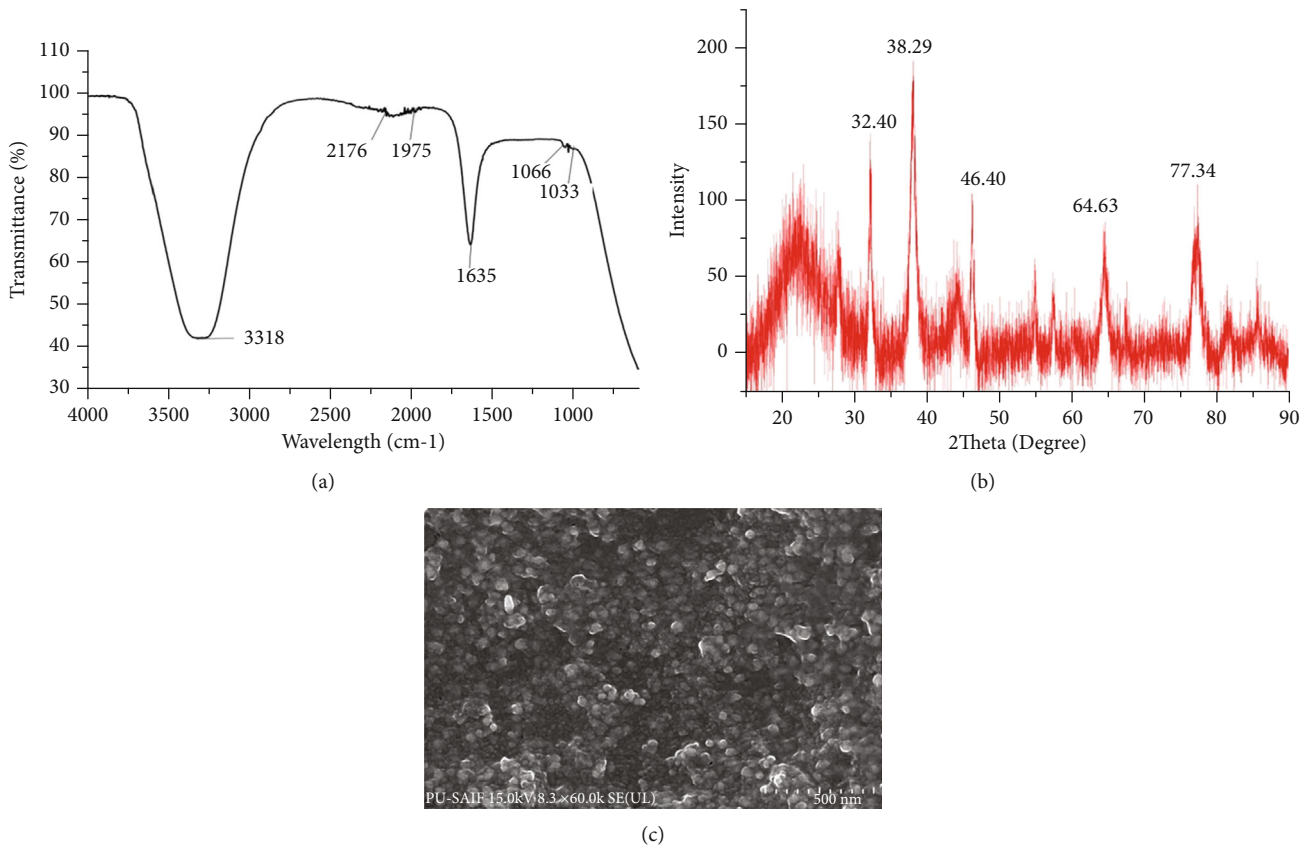

Figure 1: Characterization of biosynthesized AgNPs. (a) FTIR spectra. (b) XRD spectrum. (c) SEM micrographs.

3.2. Thickness. The PS-based films' film thickness with various AgNP solution contents was evaluated, and results are illustrated in Figure 2(a). The film thickness of PS and PS with AgNP solution varied from 0.3 mm to 0.7 mm. The film thickness of the PS-based films was lifted by adding an AgNP solution. Our findings agree with the study of Coelho et al. [22], which mentioned that the film thickness was enhanced as the concentration of cellulose nanoparticles derived from grape pomace is increased. A significant change in the film thickness was observed by incorporating AgNP solution, which might be related to its nature and composition (AgNPs and RE). In addition, as the AgNP solution added to the films, solid mass in the film's network also enhanced, which also promotes the film thickness. A similar discussion was presented by Martínez-Molina et al. [16] for the films made with chitosan Moringa oleifera leaf extract. Similarly, Ortega et al. [23] demonstrated that film thickness might be related to the nature and small nanoparticle aggregation in the starch matrix.

3.3. Moisture Content. The suitability of food packaging materials for the different environmental conditions depends on the MC level, and the results are exhibited in Figure 2(a). The pure PS film was $15.12 \pm 0.78\%$, which was found to decrease with the increase in AgNP solution. A marked difference ($P < 0.05$) in MC of the PS films and PS films with AgNP solution was observed. Our result is in line with the earlier work in which the MC of chitosan/gelatin films decreased with the increasing concentration of AgNPs [24]. Similarly, Mohammadian et al. registered that the MC of the whey protein film was greatly diminished by enriching nettle leaf extract [25]. Reduction in the MC with the addition AgNP solution is related to the hydrogen bonds with starch's hydrophilic sites, limiting the interaction among the starch and water molecules [26].

3.4. Swelling Index. The film's water sorption ability is dependent on the polymer's hydrophilicity property and compactness. Changes in SI values with AgNP solution are illustrated in Figure 2(b). According to Figure 2(b), the pure PS film was soaked more water than PS-based film-loaded AgNP solution. SI values declined significantly ($P < 0.05$) when AgNP solutions were added, caused by attaching hydroxyl groups in starch with water. A similar phenomenon was noticed in the study of chitosan/ZnO nanocomposite films [27]. Similar trends and discussions were also reported in published work [28]. AgNP solution in the films blocked the hydrophilic sites due to its hydrophobic nature. Consequently, free hydrophilic sites' availability for water interaction was reduced, decreasing the SI [29].

3.5. Opacity. The OP is a crucial feature of packaging films that protect light-sensitive food materials from UV and light radiation. Moreover, it also influences the market and customer acceptability of food materials. Figure 2(b) presents the OP values of the PS-based film and active films. The OP of the PS-based films enhanced follows the incorporation of

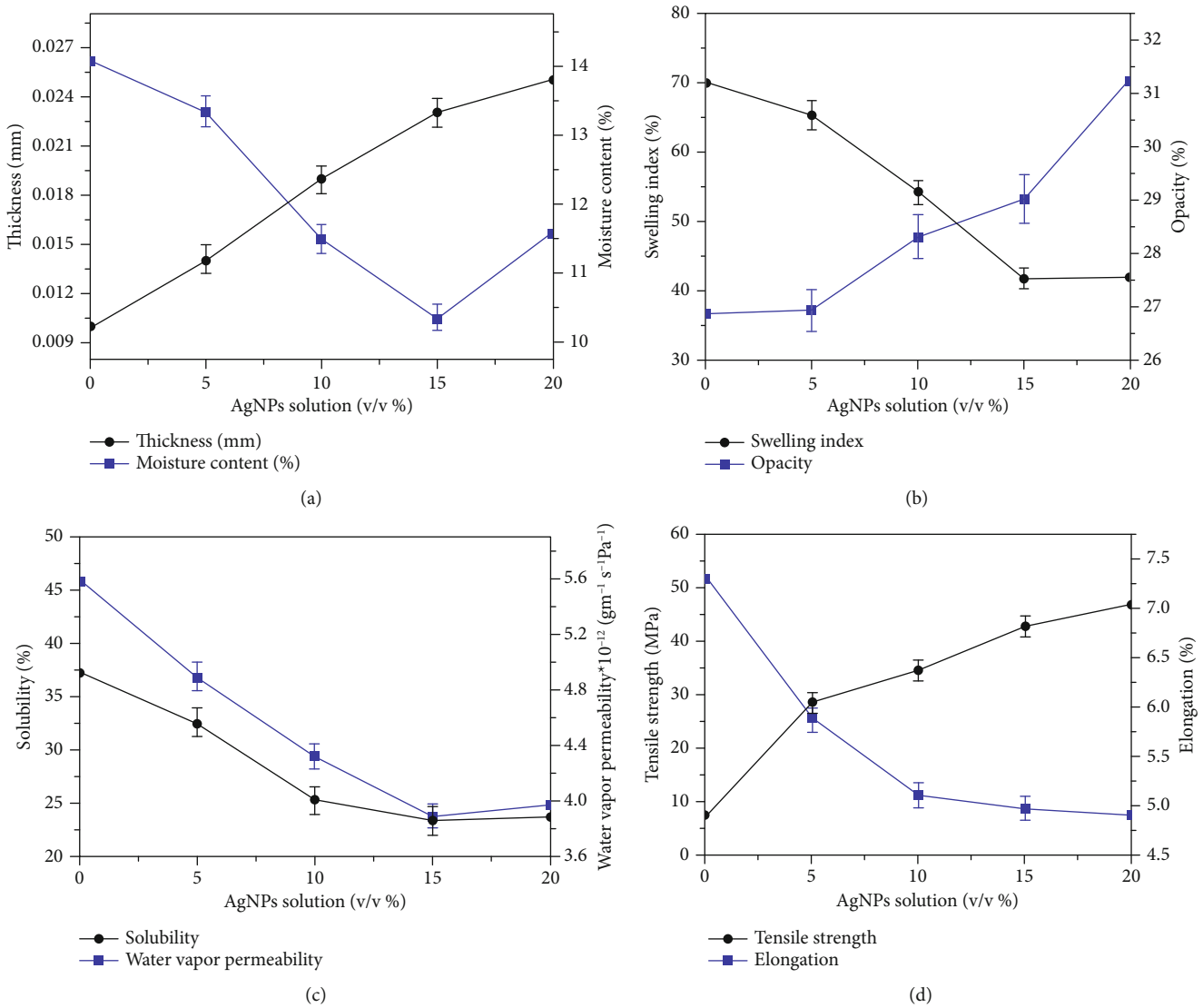

Figure 2: Impact of AgNP solution. (a) Thickness & MC, (b) SI & OP, (c) WS & WVP, and (d) MS and *E*.

AgNP solution, which might be related to the active functional groups in the AgNP solution. However, the AgNP solution in the PS matrix significantly ($P < 0.05$) altered the film's opacity. Kang et al. [30] described the films made with gum arabic and cellulose nanocrystal. They showed that the nanocomposite films' OP improved following the addition of nanocrystal. Andrade-Pizarro et al. [31] reported similar explanations and trends, where the cellulose nanofibrils improved the optical property of the gelatin film. Improvement in the film's OP could be related to diffusion in light reflection by sunk AgNP solution in the PS-based film [32].

3.6. Solubility. The WS values of the neat PS and PS-based films with AgNP solution are exhibited in Figure 2(c). From the results, the WS of the active film revealed an increase in most of the films with AgNP solution. PS film has the highest WS values than active films, and solubility declines with the increase in AgNP solution content. Furthermore, WS values of the active films slightly dropped if the AgNP solution amount was added more than 15 *v*/*v* %. Few studies showed that the cellulose nanocrystal in starch films decreased the WS than neat starch films [22]. The results revealed a remarkable ($P < 0.05$) decrease in the active films' WS compared to the PS neat film. Kochkina and Butikova [7] discussed similar findings and trends, who found a decrease in the solubility of gelatin films added with AgNPs, and Ortega et al. [24] noticed a decrease in the solubility of the starch film added with AgNPs. Hydrophobic components in AgNP solution can develop the interaction with starch chains and alter the nature of the films, resulting in the development of active films with lower solubility [26].

3.7. Water Vapor Barrier Property. WVP plays a pivotal role in preserving the food quality and shelf life during storage and transportation. It should be as low as possible. WVP values of the neat PS-based films and active films are displayed in Figure 2(c). PS film reveals the highest WVP values compared to the active films, thereby matching the trend

and discussion with earlier work reported by Yan et al. [32]. A synergistic ($P < 0.05$) change was observed in WVP values of the PS-based film and active film. A similar explanation and trend were discussed in a published work by Rhim et al. [33], who stated that WVP values of the films diminished with nanoparticles. However, the WVP of the films slightly enhanced with further incorporation of AgNP solution, which might be related to aggregation AgNPs in the polymer matrix, causing alteration in the matrix channels [34]. The possible explanation could be that RE improved the PS films' crystallinity, reducing the WVP [35].

3.8. Mechanical Property. The MS and *E*% values of the PS-based films with varied AgNP solutions are illustrated in Figure 2(d). When various AgNP solution content was added, MS of the film enhanced significantly ($P < 0.05$). While the *E*% at the breaking point of the films decreased, which may be associated with compactness/toughness in the films, it prohibited the motion among the starch chains [36]. However, with enhancing the contents of the AgNP solution, MS showed a first increasing and decreasing trend. Besides, the nanocomposite films still showed good flexibility compared to PS films. Meanwhile, the AgNP solution in the PS-based film was able to improve almost all essential functional properties (Figure 2(d)). Similarly, other literature on AgNPs to agar [33] and gelatin [37] reported similar outcomes and trends. Enhancement of the MS of the films was probably associated with bioactive compounds present in the extract and nanoscale of AgNPs, which limits the motions of polymer chains in the films [38].

3.9. Hydrophilicity. The contact angle is the best way to express the hydrophilic and hydrophobic nature of the PS-based films and active films. Variation in CA with the various AgNP solution in the active films is shown in Figure 3. Generally, a small contact angle demonstrates high hydrophilicity of the surface and vice versa. In Figure 3, neat PS film exhibits the lowest CA, indicating a highly hydrophilic surface. With the addition of AgNP solution, the CA of the PS films enhanced, which shows that the moisture absorption capacity of the PS films diminished. Similar outcomes were suggested by [39] about the effect of the TiO_2 content on the hydrophilic nature of the starch film surface. Outcomes in this work exhibited that increasing the AgNP solution in the PS matrix improved the CA of the PS films significantly ($P < 0.05$). The improvement in the CA of PS films was due to excellent combinations among the components of the AgNP solution with the PS matrix. In other words, the elements of AgNP solutions altered the nature of the PS films from being hydrophilic to being hydrophobic, mainly due to the excellent dispersion of the components of AgNP solution in the PS matrix [40].

3.10. UV–vis Spectroscopy. The protection of food materials against UV light is important for prevention of color change, undesirable order, and lipid oxidation [41]. UV-vis spectra in the wavelength range from 200 to 700 nm of the PS-based film and active film are revealed in Figure 4. As exhibited in Figure 4, the transmittance of the PS film in the visible region diminished with the increase of the content of the AgNP solution. A remarkable change in the absorption of a neat PS-based film and active film in the visible and UV region was noticed. The light absorption at 280 nm of PS films increased linearly with the AgNP solution. A decrease in the UV transmittance at 280 nm of the active film was seen because of the phenolic compounds present in the AgNP solution, which are recognized to have UV light absorption capacity as noticed in the agar films added with banana powder exhibiting UV transmittance [42]. A similar trend and observation were observed [43]. However, absorption of PS-based films enhanced with AgNP solution in the wavelength range from 200 nm to 800 nm. But the difference in peak intensity between PS and PS-based films with AgNP solution associated AgNP solution content in the UV-B region (280 nm to 315 nm). PS-based films with AgNP solution revealed the highest absorption at the AgNP solution content (15% *v*/*v*). This might occur due to phenolic groups or AgNPs in the plant extract [12].

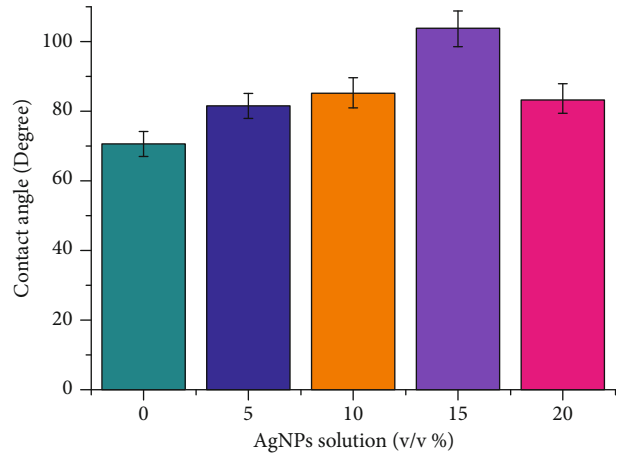

Figure 3: Effect of AgNP solution on the hydrophilicity of the films.

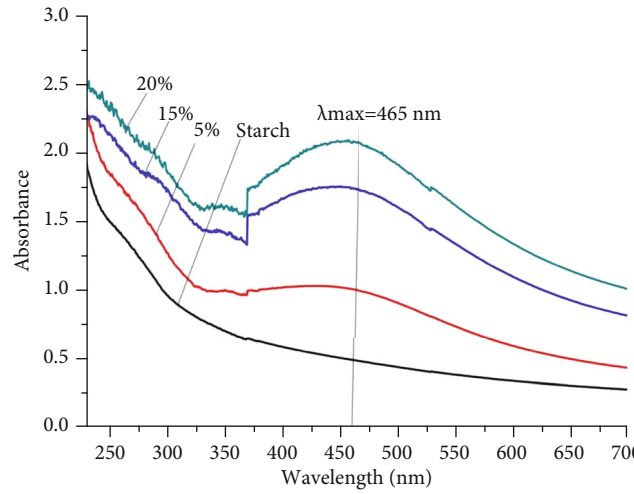

Figure 4: Influence of AgNP solution on UV resistance capacity of the films.

3.11. FTIR Analysis. The FTIR spectra of neat PS and active films are shown in Figures 5(a) and 5(b). The wide peaks

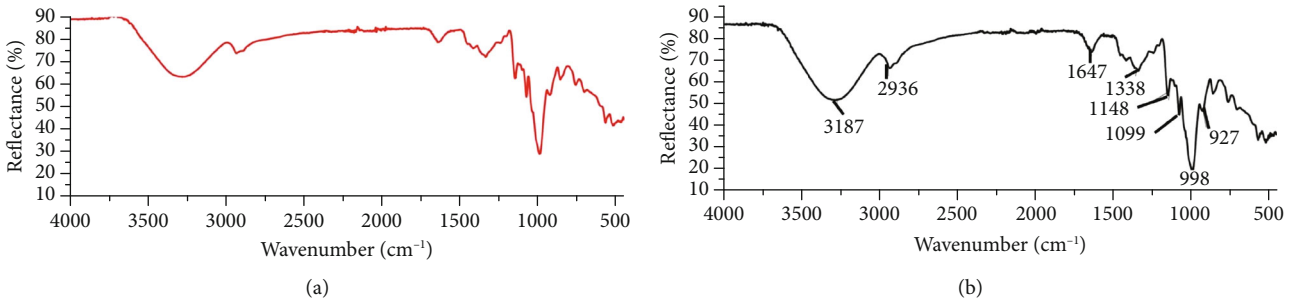

Figure 5: FTIR spectra of the (a) active film and (b) PS-based film.

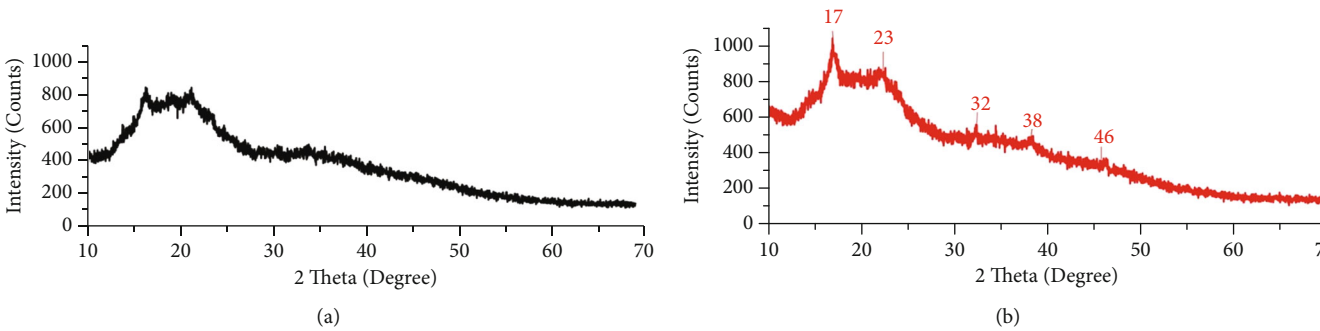

Figure 6: XRD spectra of the (a) PS-based film and (b) active film.

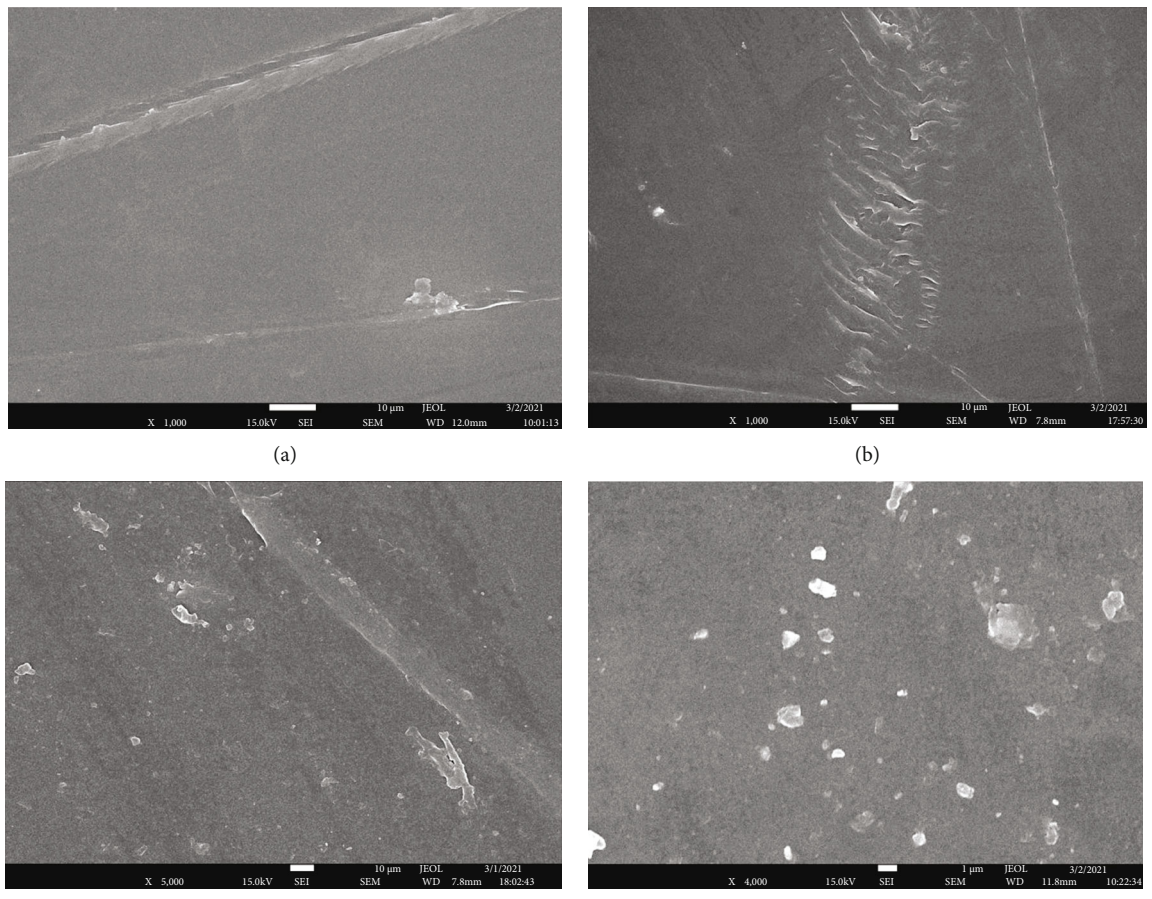

Figure 7: SEM images of the (a, b) active film and (c, d) PS-based film.

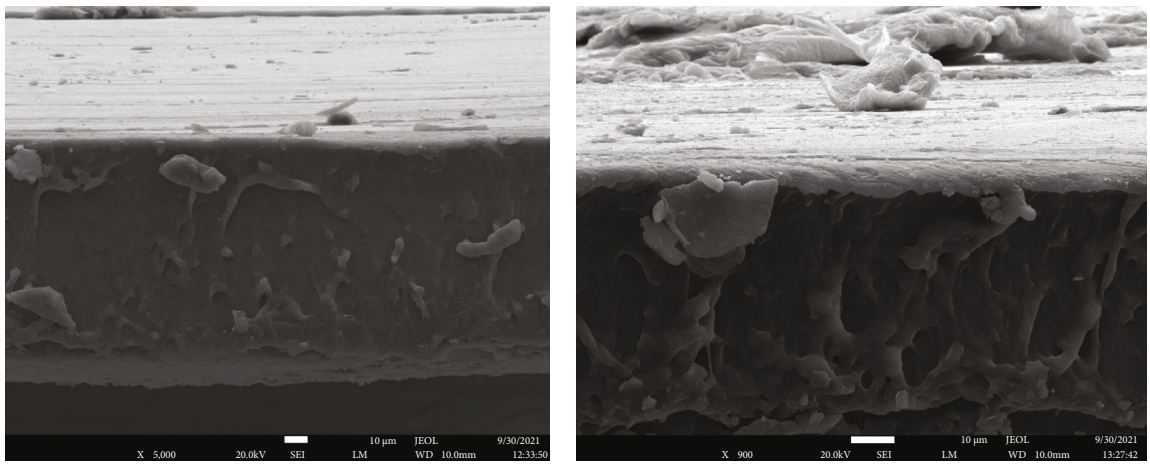

(a) (b)

Figure 8: Cryofracture SEM images of nanocomposite films.

around 3200 cm^{-1} noticed in both PS-based film and active films were due to interactions among the functional groups of PS and sorbitol (–OH stretching). Another peak which was around 2900 cm^{-1} was due to –C-H stretching vibration. The peaks around 1650 cm^{-1} are due to the presence of moisture content in the films. Similar findings and discussions were reported by [44]. The peak at 1065 cm^{-1} represents the C-O bond stretching of C-O-C groups [45]. The peaks at 1338–1148 cm^{-1} are related to C-OH or amine groups. The peaks in the range of 800–1000 cm^{-1} matched with C-H stretching of residual plasticizer molecules. Compared with PS films, a similar pattern with only high or low band intensity was observed in the PS-based film with AgNP solution films (Figure 5(a)). The FTIR outcomes were similar for both PS films with and without AgNP solution which shows that the chemical structure of the PS did not vary by the addition of AgNP solution. Changes in the peak intensity of PS-based films could be due to physical interactions in hydrogen bonding or van der Waals force among AgNP solution and the PS matrix [46].

3.12. XRD Analysis. The XRD approach is carried out to understand the possible changes that occurred in the crystallinity of the film following the addition of AgNP solution (Figures 6(a) and 6(b)). The XRD result of neat PS-based films illustrates broad peaks around 16° and 22°, connected with the semicrystalline network of PS. In addition, the XRD pattern for green synthesized AgNPs, reported in earlier work [18], where peaks at 2θ of 38°, 44°, 64°, 77°, and 81°, were noticed. Figure 6(b) represents the XRD pattern for PS films enriched with AgNP solution. New characteristic peaks were seen at 32°, 36°, and 46° in the PS-based films with AgNP solution. Similar outcomes were suggested when the AgNP content was added in the alginate films [47]. Compared with the neat PS-based films, PS-based films with AgNP solution peaks were broader, associated with the size quantization impact of AgNP. Moreover, a slight shift in the peak position of PS-based films was noticed upon addition of AgNP solution. An increased peak intensity PS-based film with AgNP solution showed an increase in structure compactness and, consequently, an enhancement in film crystallinity [44].

Table 1: Antibacterial activity of the AgNP and film-forming solution.

Strains	*P. aeruginosa*	*S. aureus*
AgNPs	*12*	*7*
Active film-forming solution	10	6
Rifampicin (positive control)	5	39

3.13. SEM Analysis. The SEM technique is used to understand the compatibility between AgNP solution and PS in the film. Moreover, it gives the picture of how AgNP solution is distributed in the polymer matrix and results are displayed in Figures 7(a)–7(d) and 8). No synergistic variation in the morphology of all films was observed when AgNP solution was added. However, some scratches on the surface of the films were noticed, which might be occurring during the peeling process. Similarly, Roy et al. [48] confirmed that the agar-based film becomes more coarse and heterogeneous with the simultaneous addition of the copper sulfide nanoparticles. The surface of the PS film is slightly smoother than active films. However, no cracks were noticed in all the active films. AgNPs are highly compatible with the PS matrix, promoting the effective stress transfer of the load to the prepared films. Furthermore, to evaluate the level of Ag particle distribution in the starch matrix, we have taken the SEM imaging from the cryofracture surface area. Figures 8(a) and 8(b) display the resulting cryofracture SEM images of nanocomposite films in addition from the film surface. The outcomes obtained from the active films are in good accord with those described earlier in the literature [49]. The surface roughness of the film could be related to high interfacial interactions and the AgNP immobilization effect on the PS matrix [50].

3.14. Antibacterial Activity. The antibacterial activity of the film-forming solution was tested against *P. aeruginosa* and

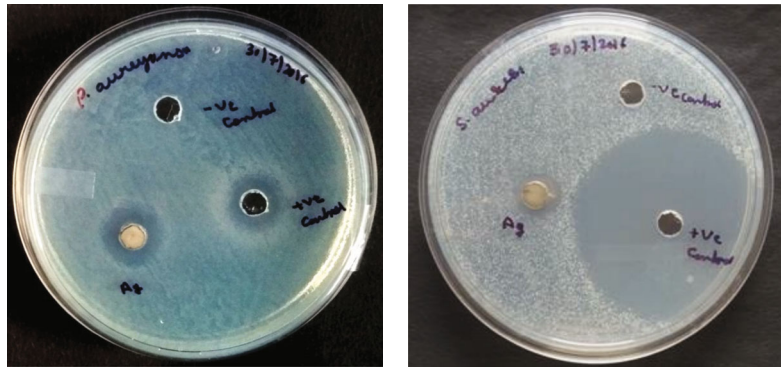

(a) (b)

Figure 9: Antibacterial activity of film solution against *P. aeruginosa* and *S. aureus*.

S. aureus microorganisms and outcomes are shown in Table 1 and Figure 9. Our results displayed that the film-forming solution demonstrated enhanced antibacterial activity against *P. aeruginosa* and *S. aureus* when compared with control. Moreover, the film-forming solution displayed a better inhibition zone against *P. aeruginosa* than *S. aureus*. Similarly, Mohammadian et al. [25] reported that active films made with whey protein and nettle leaf extract presented excellent antibacterial activity against *Staphylococcus aureus* and *Escherichia coli*. Lim et al. [51] also suggested that the antibacterial activity of the alginate-based edible film was most likely related to its flavonoids in the hawthorn berry extract. A possible working mechanism of the film-forming solution with AgNPs might be linked to silver ions. These silver ions have the ability to get connected to cell surfaces thereby disrupting the cell membrane, leading to cell death [52].

4. Conclusion

The AgNP solution synthesis is considered an eco-friendly approach due to its nontoxic by-products and chemical reaction. So, the current research is aimed at utilizing *Syzygium samarangense* extract for the eco-friendly production of AgNP solution. According to the solution casting technique, active films were synthesized from PS and AgNP solution. Our results disclosed that the active films embedded with 15% AgNPs showed enhanced physicochemical properties such as MC, WS, SI, WVP, OP, and TS. FTIR results showed that AgNP solution in the PS matrix induced strong interactions. Furthermore, SEM images displayed that after incorporation of AgNP solution, active films become more compact and homogenous throughout. The active films with AgNP solution also exhibited excellent antibacterial properties against *P. aeruginosa* than *S. aureus*.

Data Availability

The data supplied to support the outcomes of this work are included in the article.

Conflicts of Interest

There are no conflicts of interest among the authors.

Authors' Contributions

Raj Kumar, Naina Gautam, Shashikant Yadav, Venketesh T, and Nasir Awol contributed equally to this work.

Acknowledgments

The authors are thankful to National Institute for Interdisciplinary Science and Technology (CSIR), Trivandrum, India; CSIR-Central Building Research Institute, Roorkee, Uttrakhand 247667, India; Dr. B. R. Ambedkar National Institute of Technology, Grand Trunk Road, Barnala-Amritsar Bypass Rd., Jalandhar, Punjab 144011, India; and Hawassa University, college of natural and computational science, department of physics, Hawassa, Ethiopia, for providing the research facilities.

References

[1] F. Muratore, S. E. Barbosa, and R. E. Martini, "Development of bioactive paper packaging for grain-based food products," *Food Packaging and Shelf Life*, vol. 20, p. 100317, 2019.

[2] G. Zhao, C. Zhou, and F. Fan, "Preparation and properties of soy protein isolate/cotton-nanocrystalline cellulose films," *International Journal of Polymer Science*, vol. 2021, 7 pages, 2021.

[3] U. Shah, A. Gani, B. A. Ashwar et al., "A review of the recent advances in starch as active and nanocomposite packaging films," *Cogent Food & Agriculture*, vol. 1, no. 1, pp. 1–9, 2015.

[4] N. Awol, C. Amente, G. Verma, and J. Y. Kim, "Morphology and surface analyses for CH3NH3PbI3perovskite thin films treated with versatile solvent-antisolvent vapors," *RSC Advances*, vol. 11, no. 29, pp. 17789–17799, 2021.

[5] H. Gao, J. Rao, Y. Guan et al., "Investigation of the thermo-mechanical properties of blend films based on hemicelluloses and cellulose," *International Journal of Polymer Science*, vol. 2018, 10 pages, 2018.

[6] A. Arora and G. W. Padua, "Review: nanocomposites in food packaging," *Journal of Food Science*, vol. 75, no. 1, pp. R43–R49, 2010.

[7] N. E. Kochkina and O. A. Butikova, "Effect of fibrous TiO_2 filler on the structural, mechanical, barrier and optical characteristics of biodegradable maize starch/PVA composite films," *International Journal of Biological Macromolecules*, vol. 139, pp. 431–439, 2019.

[8] D. S. More, M. J. Moloto, N. Moloto, and K. P. Matabola, "Silver/copper nanoparticle-modified polymer chitosan/PVA blend fibers," *International Journal of Polymer Science*, vol. 2021, 12 pages, 2021.

[9] A. S. A. Al-Sherbini, H. E. A. Ghannam, G. M. A. El-Ghanam, A. A. El-Ella, and A. M. Youssef, "Utilization of chitosan/Ag bionanocomposites as eco-friendly photocatalytic reactor for bactericidal effect and heavy metals removal," *Heliyon*, vol. 5, no. 6, p. e01980, 2019.

[10] H. S. El-Sayed, S. M. El-Sayed, A. M. M. Mabrouk, G. A. Nawwar, and A. M. Youssef, "Development of eco-friendly probiotic edible coatings based on chitosan, alginate and carboxymethyl cellulose for improving the shelf life of UF soft cheese," *Journal of Polymers and the Environment*, vol. 29, no. 6, pp. 1941–1953, 2021.

[11] N. Awol, C. Amente, G. Verma, and J. Y. Kim, "A versatile lead iodide particle synthesis and film surface analysis for optoelectronics," *Journal of Alloys and Compounds*, vol. 829, article 154486, 2020.

[12] R. Kumar, G. Ghoshal, and M. Goyal, "Effect of basil leaves extract on modified moth bean starch active film for eggplant surface coating," *LWT*, vol. 145, p. 111380, 2021.

[13] N. S. Saada, G. Abdel-Maksoud, M. S. Abd El-Aziz, and A. M. Youssef, "Green synthesis of silver nanoparticles, characterization, and use for sustainable preservation of historical parchment against microbial biodegradation," *Biocatalysis and Agricultural Biotechnology*, vol. 32, p. 101948, 2021.

[14] S. Roy and J. W. Rhim, "New insight into melanin for food packaging and biotechnology applications," *Critical Reviews in Food Science and Nutrition*, pp. 1–27, 2021.

[15] N. A. Al-Tayyar, A. M. Youssef, and R. R. Al-Hindi, "Edible coatings and antimicrobial nanoemulsions for enhancing shelf life and reducing foodborne pathogens of fruits and vegetables: a review," *Sustainable Materials and Technologies*, vol. 26, p. e00215, 2020.

[16] E. C. Martínez-Molina, Y. Freile-Pelegrín, S. L. Ovando-Chacón et al., "Development and characterization of alginate-based edible film from Sargassum fluitans incorporated with silver nanoparticles obtained by green synthesis," *Journal of Food Measurement and Characterization*, 2022.

[17] N. Gautam, S. Garg, and S. Yadav, "Underutilized finger millet crop for starch extraction, characterization, and utilization in the development of flexible thin film," *Journal of Food Science and Technology*, 2021.

[18] R. Kumar, G. Ghoshal, A. Jain, and M. Goyal, "Rapid green synthesis of silver nanoparticles (AgNPs) using (Prunus persica) plants extract: exploring its antimicrobial and catalytic activities," *Journal of Nanomedicine & Nanotechnology*, vol. 8, no. 4, 2017.

[19] O. O. Oluwaniyi, H. I. Adegoke, E. T. Adesuji et al., "Biosynthesis of silver nanoparticles using aqueous leaf extract of Thevetia peruviana Juss and its antimicrobial activities," *Applied Nanoscience*, pp. 903–912, 2016.

[20] S. K. Srikar, D. D. Giri, D. B. Pal, P. K. Mishra, and S. N. Upadhyay, "Green synthesis of silver nanoparticles: a review," *Green and Sustainable Chemistry*, pp. 34–56, 2016.

[21] A. Saravanakumar, M. Ganesh, J. Jayaprakash, and H. Tae, "Biosynthesis of silver nanoparticles using _Cassia tora_ leaf extract and its antioxidant and antibacterial activities," *Journal of Industrial and Engineering Chemistry*, vol. 28, pp. 277–281, 2015.

[22] C. C. de Souza Coelho, R. B. Silva, C. W. Carvalho et al., "Cellulose nanocrystals from grape pomace and their use for the development of starch-based nanocomposite films," *International Journal of Biological Macromolecules*, vol. 159, pp. 1048–1061, 2020.

[23] F. Ortega, L. Giannuzzi, V. B. Arce, and M. A. García, "Active composite starch films containing green synthetized silver nanoparticles," *Food Hydrocolloids*, vol. 70, pp. 152–162, 2017.

[24] S. Kumar, A. Shukla, P. P. Baul, A. Mitra, and D. Halder, "Biodegradable hybrid nanocomposites of chitosan/gelatin and silver nanoparticles for active food packaging applications," *Life*, vol. 16, pp. 178–184, 2018.

[25] M. Mohammadian, A. D. Moghaddam, A. Sharifan, P. Dabaghi, and S. Hadi, "Structural, physico-mechanical, and bio-functional properties of whey protein isolate-based edible films as affected by enriching with nettle (Urtica dioica L.) leaf extract," *Journal of Food Measurement and Characterization*, vol. 15, no. 5, pp. 4051–4060, 2021.

[26] S. Jafarian, S. Zomorodi, and L. R. Nasiraei, "Fabrication and characterization of an active bionanocomposite film based on basil seed mucilage and ZnO nanoparticles," *Journal of Food Measurement and Characterization*, vol. 14, no. 6, pp. 3542–3550, 2020.

[27] J. Liu, J. Huang, Z. Hu et al., "Chitosan-based films with antioxidant of bamboo leaves and ZnO nanoparticles for application in active food packaging," *International Journal of Biological Macromolecules*, vol. 189, pp. 363–369, 2021.

[28] P. Balakrishnan, N. Kalarikkal, S. Thomas, V. Kokol, and T. Volova, "Physicochemical, mechanical, barrier and antibacterial properties of starch nanocomposites crosslinked with pre-oxidised sucrose," *Industrial Crops and Products*, vol. 130, pp. 398–408, 2019.

[29] S. Shankar, L. F. Wang, and J. W. Rhim, "Preparations and characterization of alginate/silver composite films: effect of types of silver particles," *Carbohydrate Polymers*, vol. 146, pp. 208–216, 2016.

[30] S. Kang, Y. Xiao, X. Guo, A. Huang, and H. Xu, "Development of gum arabic-based nanocomposite films reinforced with cellulose nanocrystals for strawberry preservation," *Food Chemistry*, vol. 350, p. 129199, 2021.

[31] R. D. Andrade-Pizarro, O. Skurtys, and F. Osorio-Lira, "Effect of cellulose nanofibers concentration on mechanical, optical, and barrier properties of gelatin-based edible films," *DYNA*, vol. 82, no. 191, pp. 219–226, 2015.

[32] J. Yan, R. Cui, Z. Tang et al., "Development of pH-sensitive films based on gelatin/chitosan/nanocellulose and anthocyanins from hawthorn (Crataegus scabrifolia) fruit," *Journal of Food Measurement and Characterization*, vol. 15, no. 5, pp. 3901–3911, 2021.

[33] J. W. Rhim, L. F. Wang, and S. I. Hong, "Preparation and characterization of agar/silver nanoparticles composite films with antimicrobial activity," *Food Hydrocolloids*, vol. 33, no. 2, pp. 327–335, 2013.

[34] R. Syafiq, S. M. Sapuan, and M. R. M. Zuhri, "Antimicrobial activity, physical, mechanical and barrier properties of sugar palm based nanocellulose/starch biocomposite films

incorporated with cinnamon essential oil," *Journal of Materials Research and Technology*, vol. 11, pp. 144–157, 2021.

[35] D. I. Chan-Matú, V. M. Toledo-López, S. Rincón-Arriaga, A. Rodríguez-Félix, and T. J. Madera-Santana, "Preparation and characterization of chitosan-based bioactive films incorporating Moringa oleifera leaves extract," *Journal of Food Measurement and Characterization*, vol. 15, no. 5, pp. 4813–4824, 2021.

[36] E. Fortunati, S. Rinaldi, M. Peltzer et al., "Nano-biocomposite films with modified cellulose nanocrystals and synthesized silver nanoparticles," *Carbohydrate polymers*, vol. 101, pp. 1122–1133, 2014.

[37] L. Loan Khanh, N. Thanh Truc, N. Tan Dat et al., "Gelatin-stabilized composites of silver nanoparticles and curcumin: characterization, antibacterial and antioxidant study," *Science and Technology of Advanced Materials*, vol. 20, no. 1, pp. 276–290, 2019.

[38] T. Gasti, V. D. Hiremani, S. S. Kesti et al., "Physicochemical and antibacterial evaluation of poly (vinyl alcohol)/guar gum/silver nanocomposite films for food packaging applications," *Journal of Polymers and the Environment*, vol. 29, no. 10, pp. 3347–3363, 2021.

[39] S. A. Oleyaei, Y. Zahedi, B. Ghanbarzadeh, and A. A. Moayedi, "Modification of physicochemical and thermal properties of starch films by incorporation of TiO_2 nanoparticles," *International Journal of Biological Macromolecules*, vol. 89, pp. 256–264, 2016.

[40] V. Goudarzi, I. Shahabi-Ghahfarrokhi, and A. Babaei-Ghazvini, "Preparation of ecofriendly UV-protective food packaging material by starch/TiO2 bio-nanocomposite: characterization," *International Journal of Biological Macromolecules*, vol. 95, pp. 306–313, 2017.

[41] R. Kumar, G. Ghoshal, and M. Goyal, "Development and characterization of corn starch based nanocomposite film with AgNPs and plant extract," *Materials Science for Energy Technologies*, vol. 3, pp. 672–678, 2020.

[42] A. Orsuwan, S. Shankar, L. F. Wang, R. Sothornvit, and J. W. Rhim, "Preparation of antimicrobial agar/banana powder blend films reinforced with silver nanoparticles," *Food Hydrocolloids*, vol. 60, pp. 476–485, 2016.

[43] N. Vigneshwaran, S. Kumar, A. A. Kathe, P. V. Varadarajan, and V. Prasad, "Functional finishing of cotton fabrics using zinc oxide-soluble starch nanocomposites," *Nanotechnology*, vol. 17, no. 20, pp. 5087–5095, 2006.

[44] Y. A. Arfat, J. Ahmed, and H. Jacob, "Preparation and characterization of agar-based nanocomposite films reinforced with bimetallic (Ag-Cu) alloy nanoparticles," *Carbohydrate Polymers*, vol. 155, pp. 382–390, 2017.

[45] R. Kumar, G. Ghoshal, and M. Goyal, "Moth bean starch (Vigna aconitifolia): isolation, characterization, and development of edible/biodegradable films," *Journal of Food Science and Technology*, vol. 56, no. 11, pp. 4891–4900, 2019.

[46] F. C. de Almeida, C. O. de Souza, B. O. Philadelpho et al., "Combined effect of cassava starch nanoparticles and protein isolate in properties of starch-based nanocomposite films," *Journal of Applied Polymer Science*, vol. 138, no. 18, pp. 50008–50016, 2021.

[47] Y. J. Bang, S. Shankar, and J. W. Rhim, "_In situ_ synthesis of multi-functional gelatin/resorcinol/silver nanoparticles composite films," *Food Packaging and Shelf Life*, vol. 22, p. 100399, 2019.

[48] S. Roy, J. W. Rhim, and L. Jaiswal, "Bioactive agar-based functional composite film incorporated with copper sulfide nanoparticles," *Food Hydrocolloids*, vol. 93, pp. 156–166, 2019.

[49] L. Dai, C. Qiu, L. Xiong, and Q. Sun, "Characterisation of corn starch-based films reinforced with taro starch nanoparticles," *Food chemistry*, vol. 174, pp. 82–88, 2015.

[50] P. Cheviron, F. Gouanvé, and E. Espuche, "Starch/silver nanocomposite: effect of thermal treatment temperature on the morphology, oxygen and water transport properties," *Carbohydrate Polymers*, vol. 134, pp. 635–645, 2015.

[51] L. I. Lim, H. L. Tan, and L. P. Pui, "Development and characterization of alginate-based edible film incorporated with hawthorn berry (Crataegus pinnatifida) extract," *Journal of Food Measurement and Characterization*, vol. 15, no. 3, pp. 2540–2548, 2021.

[52] K. Basumatary, P. Daimary, S. K. Das et al., "_Lagerstroemia speciosa_ fruit-mediated synthesis of silver nanoparticles and its application as filler in agar based nanocomposite films for antimicrobial food packaging," *Life*, vol. 17, pp. 99–106, 2018.